

Domain-adaptive Fall Detection Using Deep Adversarial Training

Kai-Chun Liu, Michael Chan, Chia-Yeh Hsieh, Hsiang-Yun Huang, Chia-Tai Chan and Yu Tsao

Abstract— Fall detection (FD) systems are important assistive technologies for healthcare that can detect emergency fall events and alert caregivers. However, it is not easy to obtain large-scale annotated fall events with various specifications of sensors or sensor positions, during the implementation of accurate FD systems. Moreover, the knowledge obtained through machine learning has been restricted to tasks in the same domain. The mismatch between different domains might hinder the performance of FD systems. Cross-domain knowledge transfer is very beneficial for machine-learning based FD systems to train a reliable FD model with well-labeled data in new environments. In this study, we propose domain-adaptive fall detection (DAFD) using deep adversarial training (DAT) to tackle cross-domain problems, such as cross-position and cross-configuration. The proposed DAFD can transfer knowledge from the source domain to the target domain by minimizing the domain discrepancy to avoid mismatch problems. The experimental results show that the average F1score improvement when using DAFD ranges from 1.5% to 7% in the cross-position scenario, and from 3.5% to 12% in the cross-configuration scenario, compared to using the conventional FD model without domain adaptation training. The results demonstrate that the proposed DAFD successfully helps to deal with cross-domain problems and to achieve better detection performance.

Index Terms—Fall detection, domain adaptation, deep adversarial training

I. INTRODUCTION

Falls are one of the main health risks to old people. The World Health Organization (WHO) has reported that about 28% of people over 65 years of age fall at least once each year [1]. The fallers might suffer from severe injuries or even death if there are no immediate medical aids available. To provide timely intervention for fallers, fall detection (FD) alarm systems have become an important research topic in assistive technology and tele-healthcare. FD alarm systems with advanced wireless sensor networks and pattern recognition techniques have the capability to detect the occurrence of fall events in daily living and inform clinical professionals of emergency events. Furthermore, such alarm systems could alleviate the psychological stress of old people and caregivers [2].

Many studies have applied wearable inertial measurement

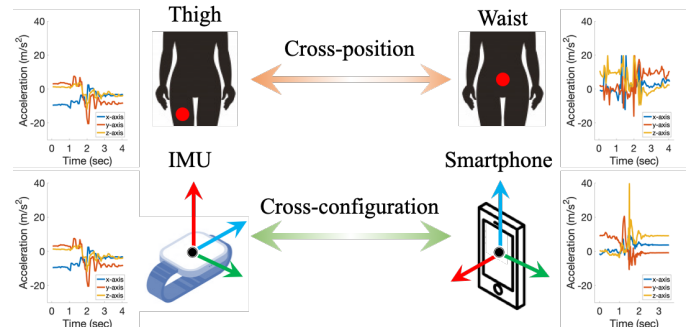


Fig. 1 Mismatch problems in real-world implementation of fall detection systems

units (IMU) to automatic FD systems [3-5] due to their various advantages, such as small size, low power, low cost, unobtrusiveness, and low invasivity. Accelerometers are the most popular measurement sensors in the field of wearable-based FD systems. They can measure the changes in body gestures and provide important movement information for FD systems. Various detection algorithms have been applied to accelerometer-based FD systems, involving threshold-based models [6], support vector machine (SVM) [7-9], k-nearest-neighbors (k-NN) [8, 9], convolutional neural networks (CNN) [10], and recurrent neural networks (RNN) [11].

Reliable FD systems utilize the training of machine learning models using well-labeled datasets. Unfortunately, it is not easy to collect sufficient datasets with various specifications of sensors or sensor positions. Moreover, the knowledge obtained through machine learning has been restricted to tasks in the same domain. The mismatch between different domains might hinder the performance of FD systems. Cross-domain knowledge transfer is very beneficial for machine-learning based FD systems to train a reliable FD model with well-labeled data in new environments. For example, the model trained on the smartphone is unsuitable for direct deployment on smartwatches because of the possible differences in sampling rate, sensing range, and resolutions.

As shown in Fig. 1, this work aims to tackle two potential cross-domain circumstances when designing FD systems for real-world applications: (i) Cross-position: Different sensor placements due to real-life requirements and individual preferences lead to diverse movement patterns. (ii) Cross-configuration: The distribution of the recorded patterns is heterogeneous under different hardware conditions (e.g., sampling rate, sensing range, resolution, and noise density), as there are various commercial sensors available in the wearable device market.

To mitigate cross-domain problems, domain-adaptation-based deep learning techniques have been developed to extract transferrable knowledge from the labeled dataset (source

Manuscript received October xx; revised xx; accepted xx. Date of publication xx; date of current version xx. This work was supported in part by grants from the Ministry of Science and Technology.

K.-C. Liu, M. Chan and Y. Tsao are with the Research Center for Information Technology Innovation (CITI) at Academia Sinica, Taipei 11529, Taiwan.

C.-Y. Hsieh, H.-Y. Huang, and C.-T. Chan are with the Department of Biomedical Engineering, National Yang-Ming University, Taipei 11221, Taiwan.

(Corresponding author: Y. Tsao, e-mail: yu.tsao@citi.sinica.edu.tw).

TABLE I
LIST OF FALL AND ADL IN UP-FALL

NO.	Type of Fall and ADL	Instances
A1	Walking	249
A2	Standing	249
A3	Sitting	249
A4	Picking up an object	249
A5	Jumping	249
A6	Laying	239
F1	Falling forward using hands	249
F2	Falling forward using knees	249
F3	Falling backwards	249
F4	Falling sideward	244
F5	Falling sitting in empty chair	249

TABLE II
LIST OF FALL AND ADL IN UMAFALL

NO.	Type of Fall and ADL	Instances
A1	Applauding	194
A2	Raising both arms	200
A3	Emulating a phone call	195
A4	Opening a door	185
A5	Sitting on a chair and getting up	86
A6	Walking	246
A7	Bending	228
A8	Hopping	206
A9	Lying down on/standing up from a bed	66
A10	Going upstairs and downstairs	142
A11	Jogging	129
F1	Forwards fall	313
F2	Backwards fall	321
F3	Lateral fall	292

domain) for use in the unlabeled dataset (target domain) [12]. These techniques have achieved successful performance in numerous research fields of speech [13] and computer vision [14]. One common domain adaptation approach is domain-adversarial training [15, 16], which aims to perform adaptive classifications based on domain-invariant feature extraction. The main idea is to train a feature extractor that could enhance a discriminator for label prediction while confusing another discriminator for domain classification.

In this work, a novel domain-adaptive fall detection (DAFD) system with a deep adversarial training (DAT) technique is proposed to tackle the domain discrepancy. The proposed DAFD system contains a CNN-based discriminative framework that can extract representative movement characteristics and critical fall features. By using the domain discriminator, the distribution of the extracted features from the source domain (i.e., waist and smartphone) aligns with that from the target domain (i.e., thigh and IMU). With DAT, the proposed DAFD could achieve better detection performance in the target domain.

The main contribution of this work is as follows:

- The proposed model could transfer knowledge from the source domain to the target domain by minimizing the domain discrepancy for cross-position and cross-configuration domain adaptation problems.
- The comprehensive performance analysis of DAFD in cross-position and cross-configuration scenarios is explored and investigated in this study.
- The reliability and effectiveness of the DAFD are validated on two emulated public fall detection datasets: UP-Fall and UMAFall datasets.
- The experimental results show that the improvement

of the average F1-score using DAFD ranges from 1.5% to 7% in the cross-position scenario and from 3.5% to 12% in the cross-configuration scenario compared to that of the conventional FD model without domain adaptation training.

The remainder of this paper is organized as follows: In Section II, we introduce the chosen open datasets and their experimental setup. Section III presents the pre-processing processes of the accelerometer signal, involving resampling, impact-defined window, and min-max normalization. Section IV describes the architecture and design mechanisms of the proposed DAFD. The experimental results using the DAFD are presented in Section V. The comprehensive performance analysis of the proposed model for FD systems, its limitations, and future works are discussed in Section VI. Finally, we conclude this work in Section VII.

II. OPEN DATASETS

There are more than ten public datasets available for the evaluation of FD algorithms in wearable-based FD systems [17]. This study utilizes UP-Fall [18] and UMAFall [19] datasets to validate the proposed DAFD systems, while the objective is to tackle the technical challenges in cross-position and cross-configuration. Compared to other datasets, these two datasets place more than four sensor nodes on different locations of the body. Moreover, the employed sensor nodes and the configuration of these two datasets are completely different. It shows that the datasets fulfill the requirements of this work.

A. UP-Fall

The UP-Fall dataset was proposed by Martínez-Villaseñor *et al.* [18]. There were 17 healthy young subjects (9 males, 8 females, 18–24 years old, mean height: 1.66 m, mean weight: 66.8 kg) with five fall types and six types of activities of daily living (ADL). Due to data loss and overflow errors, we had to exclude 20% of the data. On average, 992 fall instances and 1197 ADL instances from accelerometers were used in this work. Details of the fall and ADL types are listed in TABLE I. Five tri-axial accelerometers with a sampling rate of 18.4 Hz are placed on the neck (N), waist (WA), pocket (P), wrist (WR), and ankle (A), as shown in Fig. 2.

B. UMAFall

Another dataset, UMAFall, proposed by Santoyo-Ramón *et al.* [19] was used in this study. Four tri-axial accelerometers were placed on the chest (C), waist (WA), wrist (WR), and ankle (A), and a tri-axial accelerometer of the smartphone was placed in the pocket (P), as shown in Fig. 2. The accelerometers of IMUs and a smartphone were utilized to measure movement signals during the experiment. The sampling rates of the IMUs and the smartphone were 20 Hz and 200 Hz, respectively. The UMAFall dataset involved 19 subjects (11 males, 8 females, 19–68 years old, average height: 1.70 m, and average weight: 71.63 kg) for the experiments. However, seven of the subjects did not perform falls, and data loss and overflow errors were also found in this dataset. On average, only 740 fall instances

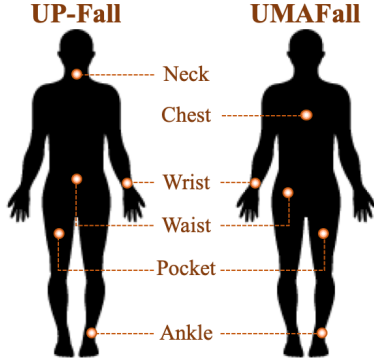


Fig. 2 An illustration of the sensor placements for UP-Fall and UMAFall datasets.

and 1501 ADL instances collected from 12 subjects were applied to this work. There was a total of 3 fall types and 11 ADL types performed in this dataset, as shown in TABLE II.

III. PRE-PROCESSING

The resampling approach is first applied to the datasets as the sampling rates of UP-Fall and UMAFall are different. It is necessary to unify the dimensions during the training and testing stages. In this work, the dataset with the higher sampling rate is downsampled to the sampling rate of the dataset with a lower sampling rate. Therefore, the UMAFall dataset with higher sampling rates (20 Hz and 200 Hz) were resampled to 18.4 Hz (sampling rate of UP-Fall dataset). A simple linear time warping resampling approach is employed in the UMAFall dataset. The UMAFall dataset is resampled by a resampling factor p/q , where p is the value after the time warping process, and q is the total number of instances in the UMAFall dataset being resampled. Such an approach is implemented using Signal Processing Toolbox in the MATLAB 2016b environment.

Next, an impact-defined window is employed for the data. Such a windowing approach has shown superior detection performance in previous studies [7-9, 20]. The main idea is to segment the data sequence based on the detection of the critical impact point during the entire fall event. The segmented data could cover several important states of the fall event, involving free-fall, vibration, and resting. The impact-defined window is determined as follows: First, the $Norm_{xyz}$ of the input three-dimensional accelerometer data $S = \{s_i | i = 1, 2, \dots, n_s\}$ is calculated:

$$Norm_{xyz}(s_i) = \sqrt{a_{x_i}^2 + a_{y_i}^2 + a_{z_i}^2}, \quad (1)$$

where n_s is defined as the total data samples of S and a_{x_i}, a_{y_i} , and a_{z_i} are the x-axis, y-axis, and z-axis samples of s_i . Then, the impact point s_p is determined as the maximum value of $Norm_{xyz}$. Finally, the impact-defined window is determined as $W_I = \{s_{I-WS_b}, \dots, s_{I-1}, s_I, s_{I+1}, \dots, s_{I+WS_f}\}$, where WS_f and WS_b are the window sizes of the forward and backward sub-windows, respectively. In this study, WS_f and WS_b are determined as 1.5 s and 2 s, while the previous study showed that FD systems with such window sizes achieve the highest

detection performance [8]. Therefore, the input is 66 (37+1+28) data samples with a sampling rate of 18.4 Hz.

After the windowing process, min-max normalization is used to reduce scaling effects on the DAFD model during the training phase. Assume a series of data $S = \{s_j | j = 1, 2, \dots, n_s\}$, where s_j can be normalized to $[0, 1]$ with min-max normalization:

$$s_j^{nom} = \frac{s_i - s_{min}}{s_{max} - s_{min}}, \quad (2)$$

where s_{max} and s_{min} are the maximum and minimum of S . In this work, min-max normalization is applied to each dimension of tri-axial accelerometers, respectively.

IV. DOMAIN-ADAPTIVE FALL DETECTION

A. Model Architecture

Given that labeled data segments $R_s = \{(r_i, l_i) | i = 1, 2, \dots, n_s\}$ collected from the source accelerometer are sufficient to perform task learning T_s for fall detection in the source domain, where r_i is the i th data sample, and $l_i \in \{ADL, Fall\}$ indicates the class of the i th data sample. Unlabeled data segments collected from the target accelerometer are denoted as $R_t = \{(r_j) | j = 1, 2, \dots, n_t\}$, where r_j is the j th data segment and n_t is the total data sample of R_t . The main goal of domain adversarial training is to perform task learning T_t for fall detection on unlabeled target data by extracting invariant knowledge from T_s , R_s , and R_t .

In this study, domain-adversarial neural network (DANN) [16] is applied to the proposed DAFD that incorporates a domain classifier and a fall detector. The architecture of the proposed DAFD using DANN is shown in Fig. 3 DANN is shown to generalize well from one domain to another while preserving low risk in the source domain in sentiment analysis and image classification tasks [16]. During the training phase, the fall detector learns the discriminative ability to identify falls and ADLs. The domain classifier contains a gradient reversal layer (GRL), which keeps the input unchanged in the forward pass and reverses the gradient during back propagation. Such operation allows extracting domain-invariant and discriminative features at the same time.

The proposed DAFD consists of three components: a feature extractor G_f , a fall detector G_{fall} , and a domain classifier G_{domain} . The dimensions of the inputs and outputs of the models are as follows:

- Input of a 3D matrix has a dimension of 66 x 3.
- Features extracted by G_f has a dimension of 10 x 4.
- Output of G_{fall} has a dimension of 2.
- Output of G_{domain} has a dimension of 2.

Each of the three components has its respective purpose:

- G_f (input; θ_f) learns a function that maps the input to the feature space.
- G_{fall} (features; θ_{fall}) learns a function that maps the features to the fall/ADL output space.
- G_{domain} (features; θ_{domain}) learns a function that maps the features to the domain output space.

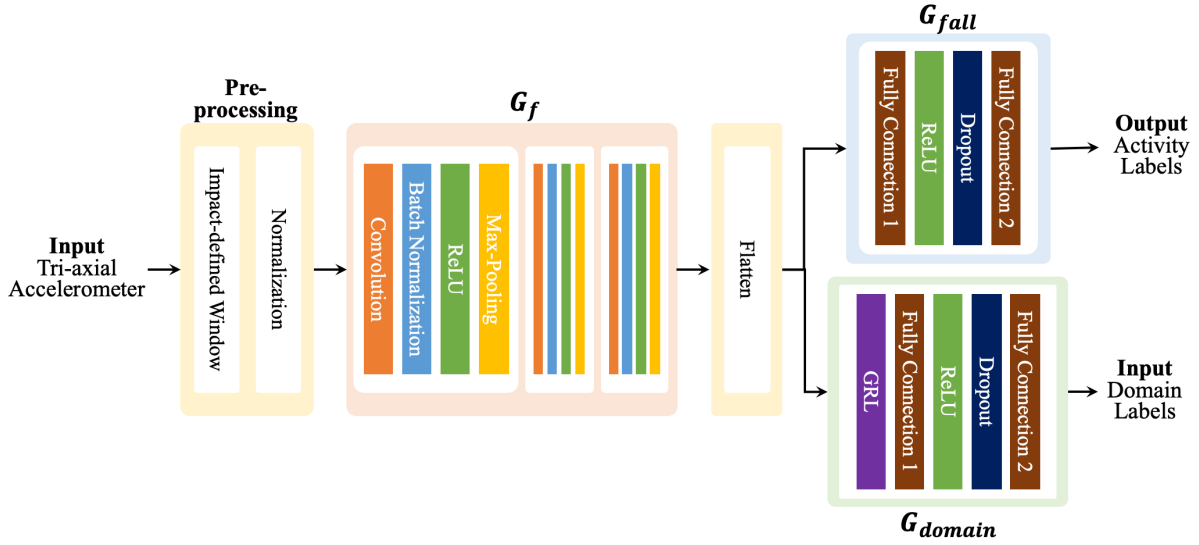


Fig. 3 Proposed adversarial training framework for domain-adaptive fall detection (DAFD).

G_f takes a batch of tri-axial accelerometer data with 66 samples per axis. G_f consists of three mixed layers. Each mixed layer comprises a convolutional layer (channel number = 4, kernel = 3, stride = 1), a batch normalization layer, a ReLU layer, and a max-pooling layer (kernel = 2, stride = 2). G_f reduces the sample size from 66 to 10 and extracts high-level features. The four channels of extracted features are then flattened into a 1D vector with a dimension of 40. Next, the extracted features are fed into G_{fall} , which includes the first fully connected layer with a dimension of 40 x 50, a ReLU layer, a dropout layer, and the second fully connected layer with a dimension of 50 x 2. While the extracted features are also fed in parallel into G_{domain} , G_{domain} is nearly identical to G_{fall} except its first layer, which is GRL. Both outputs of G_{fall} and G_{domain} are converted to probability measures through the Softmax function and finally used to compute their cross-entropy loss. Both activity labels and domain labels are binary, representing fall/ADL and source/target, respectively.

B. Parameter Training and Optimization

During the training phase, $loss_{total}$ is a summation of $loss_{fall}$ and $loss_{domain}$, which in turn corresponds to the parallelism of G_{fall} and G_{domain} . The loss function is formulated as follows:

$$loss_{total} = loss_{fall} + loss_{domain}$$

$$= \frac{1}{n_s} \sum_{i=1}^{n_s} L_{fall}(G_{fall}(G_f(r_i; \theta_f); \theta_{fall})) - \lambda \left[\frac{1}{n_s} \sum_{i=1}^{n_s} L_{domain}(G_{domain}(G_f(r_i; \theta_f); \theta_{domain})) + \frac{1}{n_t} \sum_{j=1}^{n_t} L_{domain}(G_{domain}(G_f(r_j; \theta_f); \theta_{domain})) \right] \quad (3)$$

where L_{fall} and L_{domain} are the negative log-probabilities of the correct label.

Back propagation is performed using batch gradient descent (batch size = 4 for each domain). The Adam optimizer [21] with an L2 regularization weight decay of 0.01 is used to update the

parameter with a range of learning rates (the details are introduced in Subsection C). The update rule for parameters θ_{fall} , θ_{domain} , and θ_f is described as follows:

$$\Delta\theta_{fall} = -lr * \frac{dloss_{fall}}{d\theta_{fall}}, \theta_{fall} \leftarrow \theta_{fall} + \Delta\theta_{fall} \quad (4)$$

$$\Delta\theta_{domain} = -lr * \frac{dloss_{domain}}{d\theta_{domain}}, \theta_{domain} \leftarrow \theta_{domain} + \Delta\theta_{domain} \quad (5)$$

$$\Delta\theta_f = -lr \left(\frac{dloss_{fall}}{d\theta_f} \frac{d\theta_{fall}}{d\theta_f} - \lambda \frac{dloss_{domain}}{d\theta_{domain}} \frac{d\theta_{domain}}{d\theta_f} \right), \theta_f \leftarrow \theta_f + \Delta\theta_f \quad (6)$$

where lr is the learning rate and λ is the domain regularization parameter.

Note that with this update rule, G_{fall} and G_{domain} would approach the local minimum with respect to their losses. While $loss_{fall}$ is back propagated similarly to update θ_f , $loss_{domain}$ is back propagated with an additional negative sign (an operation dictated by the GRL). θ_f is updated to reach a local maximum of $loss_{domain}$. Such adversarial training strengthens the discriminability of G_{fall} and G_{domain} , and strengthens the fall/ADL discriminability, yet weakens the domain discriminability of the features extracted by G_f .

C. Training and Validation Procedure

There are three training modes: “source only,” “DAFD,” and “target only.” For “source only,” only labeled source data is used to train the parameters of G_f and G_{fall} . $loss_{fall}$ is used during backpropagation, so the model is unaffected by $loss_{domain}$. For “DAFD,” both labeled source data and unlabeled target data are used to train the parameters of G_f , G_{fall} , and G_{domain} . Both $loss_{fall}$ and $loss_{domain}$ are used during backpropagation. For “target only,” only labeled target data is used to train the parameters of G_f and G_{fall} . Similar to the training with “source only” is only $loss_{fall}$ used during back propagation, so the model is unaffected by $loss_{domain}$. In this work, “source only” and “target only” are considered as the lower-bound and upper-bound detection performances to compare with the proposed DAFD. Because both datasets are

TABLE III
SEARCH RANGE FOR HYPERPARAMETER OPTIMIZATION

Hyperparameter	Search range
Dropout	[0.1, 0.2, 0.5]
Learning rate	[0.001, 0.0005, 0.0001]
Domain regularization parameter (λ)	[0.31, 1, 1.3]

TABLE IV
LIST OF TARGET-SOURCE PAIRS IN CROSS-POSITION AND CROSS-CONFIG. SCENARIOS

Cross-position within Dataset (Source → Target)				Cross-config. (Source → Target)	
UP-Fall		UMAFall		UP-Fall → UMAFall	UMAFall → UP-Fall
N→WA	P→WR	C→WA	WR→A	N → C	C → N
N→P	P→N	C→WR	WR→WA	WA→WA	WA → WA
N→WR	WR→N	C→A	WR→C	P→P	P → P
N→A	WR→P	WA→WR	A→C	WR→WR	WR → WR
WA→P	WR→A	WA→A	A→WA	A→A	A → A
WA→WR	WR→WA	WA→C	A→WR		
WA→A	A→WA				
WA→N	A→N				
P→A	A→P				
P→WA	A→WR				

N: neck, WA: waist, P: right pocket, WR: wrist, A: ankle, C: chest

TABLE V
OVERALL PERFORMANCE COMPARISON IN CROSS-POSITION AND CROSS-CONFIGURATION SCENARIOS (%)

		Cross-position		Cross-config. (Source → Target)	
		UP-Fall	UMAFall	UP-Fall → UMAFall	UMAFall → UP-Fall
SEN	Source only	86.62	62.72	86.08	53.06
	DAFD	89.28	72.08	92.33	67.12
	Target only	94.68	92.07	93.55	97.23
SPE	Source only	97.32	95.34	94.99	91.57
	DAFD	97.25	94.65	94.52	94.56
	Target only	98.81	95.74	98.73	99.36
PRE	Source only	96.58	89.31	90.92	86.49
	DAFD	96.55	91.61	91.41	91.78
	Target only	98.56	94.06	97.97	99.22
F1	Source only	91.24	72.31	88.24	65.63
	DAFD	92.74	80.07	91.85	77.52
	Target only	96.57	92.94	95.64	98.20

imbalanced, we implemented weighted sampling to ensure that the model has seen roughly the same amount of fall and ADL samples. Specifically, the underrepresented fall data are oversampled to reach such a goal.

Because both UMAFall and UP-Fall datasets are relatively small, 5-fold cross-validation is repeated five times to minimize the effects of cross-subject domain shifts. Furthermore, the proposed DAFD employs hyperparameter optimization and early stopping to prevent overfitting.

D. Hyperparameter Optimization and Early Stopping

The three hyperparameters selected for fine-tuning are dropout, learning rate, and domain regularization parameter (λ). Three values are picked for each hyperparameter, so there is a total of 27 permutations, as shown in TABLE III. The tuple with the lowest $loss_{total}$ is selected as the optimal hyperparameter. In addition to hyperparameter fine-tuning, early stopping is applied to prevent overfitting and to increase training speed. The criterion for early stopping is the epoch with the lowest $loss_{total}$.

The proposed model was implemented using PyTorch 1.3.1,

running on a workstation with 64-bit Ubuntu 18.04.4, Intel(R) Xeon(R) CPU E5-2683 v3 @ 2.00 GHz, and trained and tested using the Nvidia Titan Xp with 128 GB dedicated memory. The implementation of pre-processing was run in the MATLAB 2018 environment.

V. EXPERIMENTAL RESULTS

A. Cross-domain Scenario

In this study, we set up two cross-domain scenarios for the experiments. The first is cross-position, which aims to explore the capability of the proposed FD model to align data distributions collected at different body positions in the same configuration. In total, there are 20 and 12 source–target pairs for the UP-Fall and UMAFall datasets, respectively. Note that the sensor placed in the right pocket in UMAFall data is excluded in this scenario because its configuration is different from other positions. The second is cross-configuration, which explores the detection ability of the proposed DAFD to align data distributions of UMAFall and UP-Fall datasets at each sensor location. The sensors placed on the neck and chest only occur in one of the datasets, while other sensor placements overlap. Therefore, they are selected as a source–target pair in cross-configuration scenario. There is a total of 10 pairs in this scenario. All considered source–target pairs in cross-position and cross-configuration scenarios are listed in TABLE IV.

B. Evaluation Methodology

Several evaluation metrics have been involved to validate the reliability of the proposed DAFD: sensitivity (SEN), specificity (SPE), precision (PRE), and F1-score (F1). These metrics are popular performance measures in FD systems. They are defined as follows:

$$SEN = \frac{TP}{TP + FN}, \quad (7)$$

$$SPE = \frac{TN}{TN + FP}, \quad (8)$$

$$PRE = \frac{TP}{TP + FP}, \quad (9)$$

$$F1 = \frac{2 * SEN * PRE}{SEN + PRE} \quad (10)$$

where TP, TN, FP and FN are the true positive, true negative, false positive, and false negative of the labels, respectively.

C. Analysis of Classification Performance

Overall performance comparison in cross-position and cross-configuration scenarios are shown in TABLE V. The experimental results demonstrate that the detection performance of the proposed DAFD system is better than that of the source only. The improvement in all SEN and F1 ranges from 1.5% to 14%, while the SPE and PRE of several pairs remain unchanged or slightly decrease (less than 1%).

Fig. 4 and Fig. 5 show the detailed results of different source–target pairs in cross-position scenarios. The best and the worst F1-score of UP-Fall are WA→P (97.24%) and WR→A (84.63%), respectively, and those of UMAFall are C→WA (95.93%) and A→WR (60.48%), respectively. The results

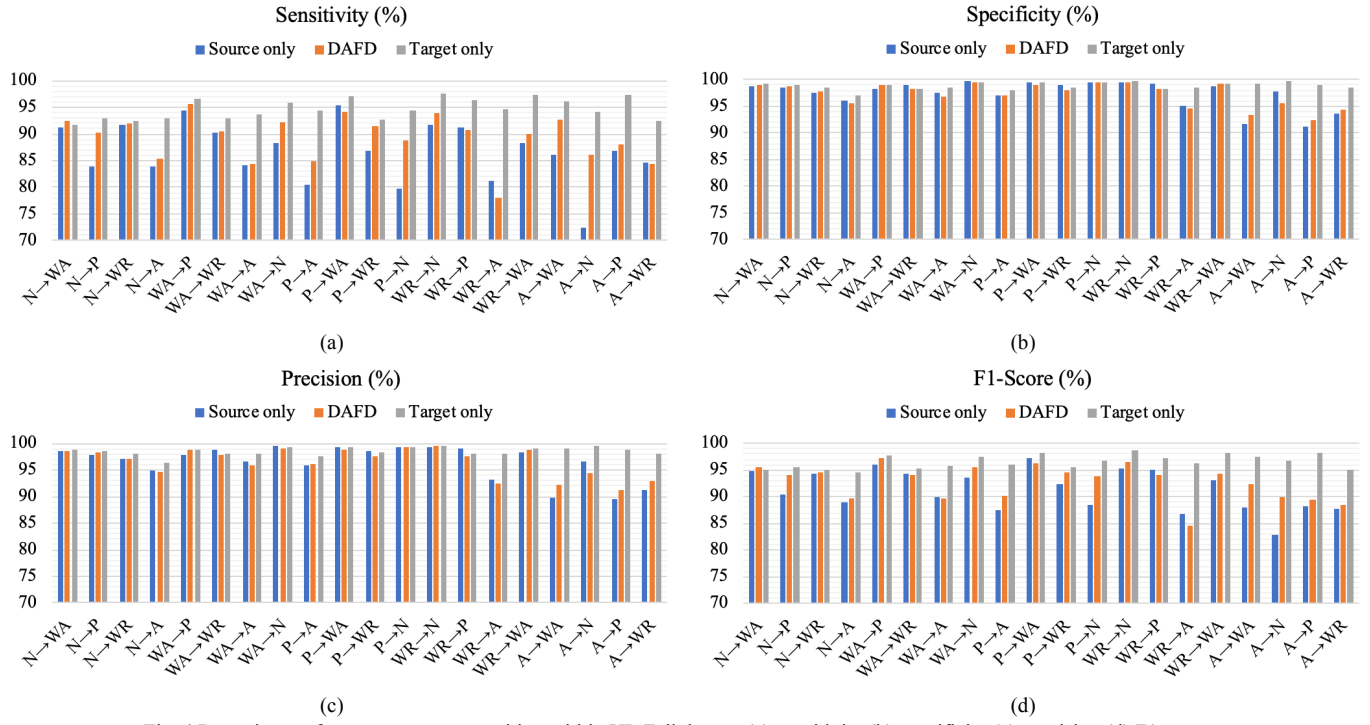


Fig. 4 Detection performance vs cross-position within UP-Fall dataset (a) sensitivity (b) specificity (c) precision (d) F1-score

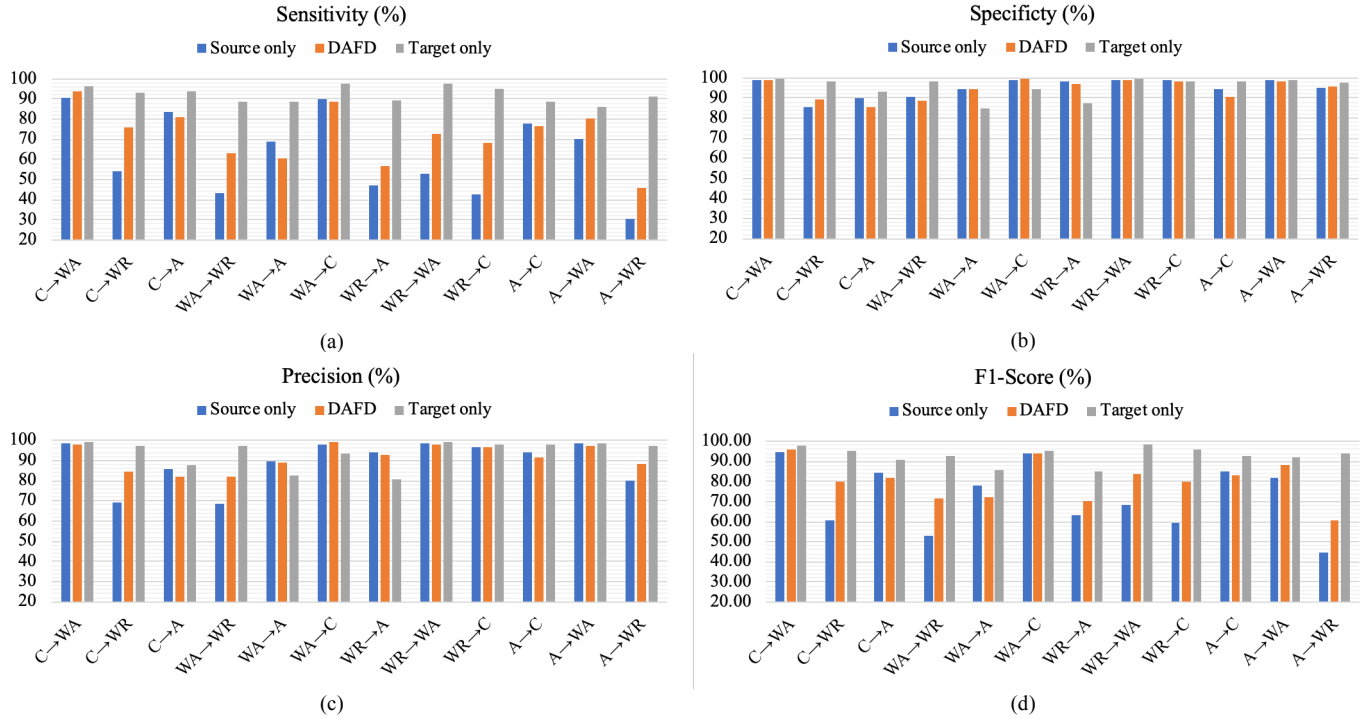


Fig. 5 Detection performance vs cross-position within UMAFall dataset (a) sensitivity (b) specificity (c) precision (d) F1-score

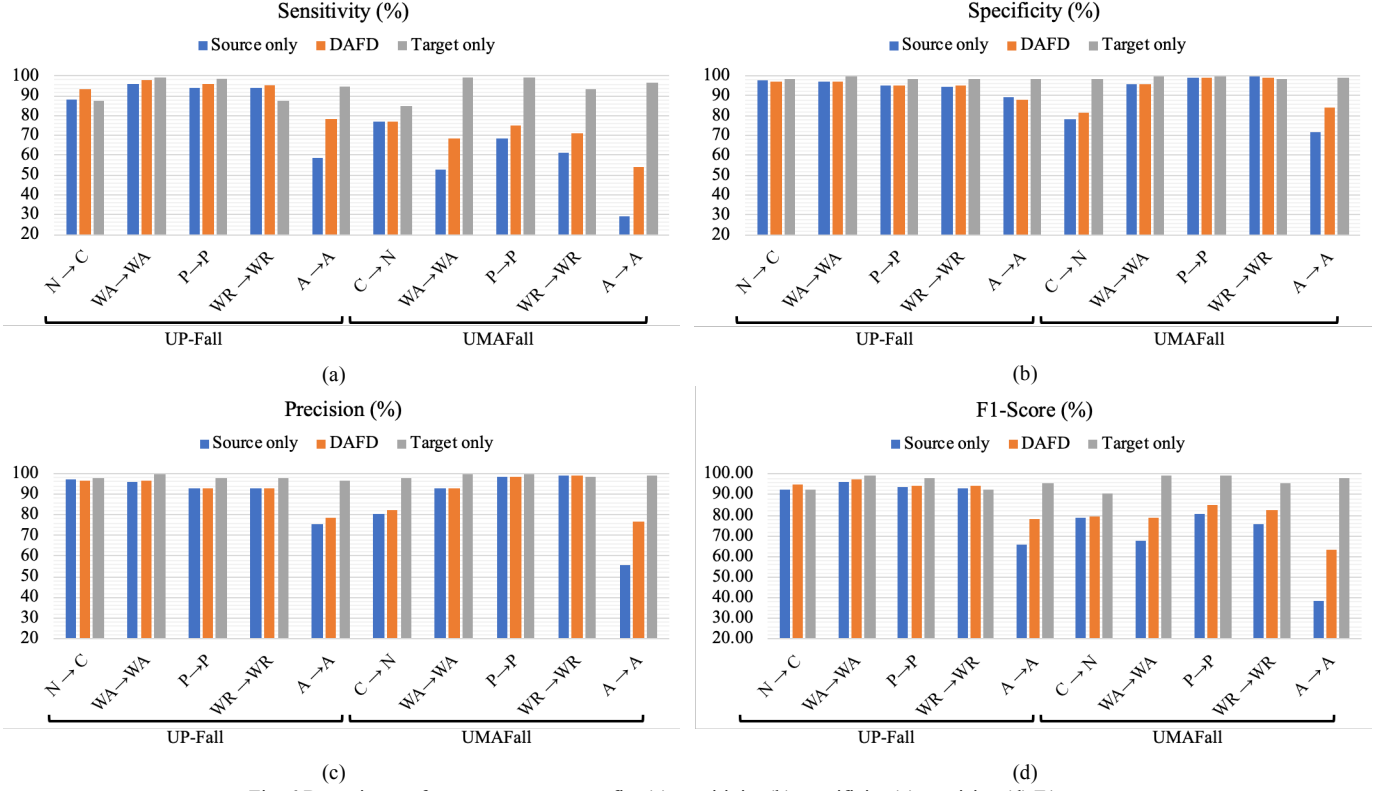


Fig. 6 Detection performance vs cross-config. (a) sensitivity (b) specificity (c) precision (d) F1-score

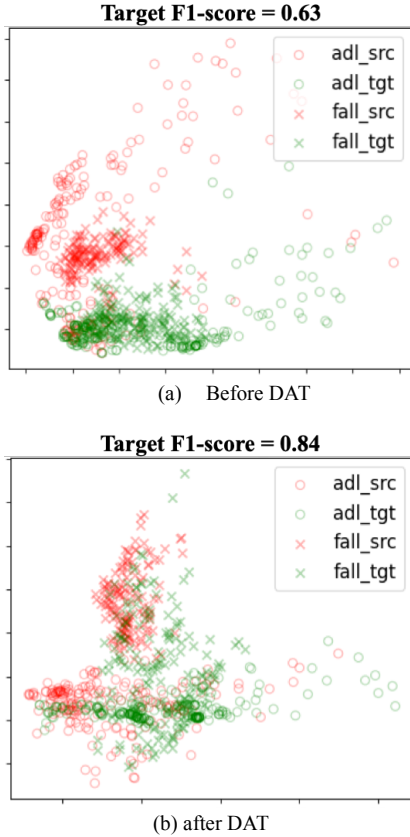


Fig. 7 Distribution of extracted features from NN using t-SNE visualization. Red and green points represent source and target domains, while cross and circle correspond to fall and ADL. (a) NN trained with “source only” (without DAT) (b) using the proposed DAFD

reveal that most positions close to the human body center, such as chest, neck, waist and pocket, can successfully adapt to each other and improve detection performance. However, the proposed DAFD fails in several source-target pairs related to the ankle and wrist, including $WA \rightarrow A$, $WA \rightarrow WR$, $WR \rightarrow P$, $WR \rightarrow A$ for UP-FALL, and $C \rightarrow A$, $WA \rightarrow A$, and $A \rightarrow C$ for UMAFall.

Fig. 6 demonstrates the detection performance in the cross-configuration scenarios. Generally, the F1 of all source-target pairs is improved with the proposed DAFD, where the improvements range from 0.75% to 24.95%. Similar to the cross-position scenario, the proposed DAFD achieves better SEN performance as the improvement of SPE and PRE are limited.

VI. DISCUSSION

In this work, DAFD using DAT is proposed to deal with realistic cross-domain problems, e.g., cross-position and cross-configuration. The overall improvements in F1 and SEN range from 1.5% to 14%. The experimental results show that the proposed approach successfully helps to tackle the problems and achieves better detection performance, especially for sensitivity.

As shown in Fig. 7, we use t-SNE [22] to visualize the distribution of the features extracted from the network. Fig. 7 (a) shows that using the “source only” training model fails to identify fall/ADL data samples of the target domain because the distribution of the target domain is different from that of the source domain. In contrast, the FD model using DAT minimizes

the discrepancy between the source and target domains, as shown in Fig. 7 (b). The proposed DAFD provides a clearer decision boundary between fall and ADL data points to the target distribution. Such results show that the proposed DAFD successfully transfers the detection knowledge from the source domain to the target domain.

Similar DAT approaches have been successfully implemented in other fields of applications, such as image processing [14] and speech processing [13]. To the best of our knowledge, this is the first study that aims to tackle cross-domain problems using DAT, while most studies still focus on improving detection performance in ideal environments.

There are several challenges that limit the detection ability of the proposed DAFD. First, the patterns collected from the sensors placed on the ankle and wrist are completely different from those on the neck, chest, waist, and pocket. It not only constrains the effectiveness of DAFD but also leads to worse performance in several source–target pairs. Second, it is challenging to train deep neural networks (DNN) with imbalanced data between fall and ADL and limited data volume from the public datasets. These problems often cause overfitting problems in the proposed FD model. Therefore, DAFD is only implemented with narrow hidden layers and small parameters of each layer. To deal with these challenges, various advanced techniques and models will be employed for DAT, involving data augmentation [23], multi-task learning [24], and few-shot learning [25].

One main limitation of this study is that we only employed the simulated datasets instead of real-world datasets (e.g., FARSEEING [26]). This is because the volume of the real-world dataset is too small to be trained with a DNN. Obviously, it requires other pre-processing techniques before using DAT, such as data augmentation and transfer learning. Additionally, several mismatch problems are not considered in this study, involving cross-age (e.g., young adults vs. elderly) and cross-sensors (e.g., accelerometer vs. gyroscope). In a future study, we plan to explore and investigate the feasibility of DAT in these cross-domain scenarios.

VII. CONCLUSION

In this study, we propose DAFD using DAT to deal with two potential cross-domain scenarios, cross-position and cross-configuration, when designing FD systems for real-world applications. The proposed model could transfer knowledge from the source domain to the target domain by minimizing the domain discrepancy for domain adaptation problems. In this study, the overall detection performance using DAFD outperforms that using typical FD systems by 1.5% to 14%. The experimental results demonstrated the feasibility and effectiveness of the proposed DAFD for tackling cross-domain problems.

REFERENCE

- [1] S. Yoshida, "A global report on falls prevention epidemiology of falls," 2007.
- [2] P. Vallabh and R. Malekian, "Fall detection monitoring systems: a comprehensive review," *Journal of Ambient Intelligence and Humanized Computing*, vol. 9, no. 6, pp. 1809-1833, 2018/11/01 2018, doi: 10.1007/s12652-017-0592-3.
- [3] C. Wang, S. J. Redmond, W. Lu, M. C. Stevens, S. R. Lord, and N. H. Lovell, "Selecting Power-Efficient Signal Features for a Low-Power Fall Detector," *IEEE Transactions on Biomedical Engineering*, vol. 64, no. 11, pp. 2729-2736, 2017, doi: 10.1109/TBME.2017.2669338.
- [4] L. Kau and C. Chen, "A Smart Phone-Based Pocket Fall Accident Detection, Positioning, and Rescue System," *IEEE Journal of Biomedical and Health Informatics*, vol. 19, no. 1, pp. 44-56, 2015.
- [5] S. Yu, H. Chen, and R. A. Brown, "Hidden Markov Model-Based Fall Detection With Motion Sensor Orientation Calibration: A Case for Real-Life Home Monitoring," *IEEE Journal of Biomedical and Health Informatics*, vol. 22, no. 6, pp. 1847-1853, 2018.
- [6] A. K. Bourke and G. M. Lyons, "A threshold-based fall-detection algorithm using a bi-axial gyroscope sensor," *Medical Engineering & Physics*, vol. 30, no. 1, pp. 84-90, 2008/01/01/ 2008.
- [7] C. Y. Hsieh, K. C. Liu, C. N. Huang, W. C. Chu, and C. T. Chan, "Novel Hierarchical Fall Detection Algorithm Using a Multiphase Fall Model," (in eng), *Sensors (Basel)*, vol. 17, no. 2, Feb 8 2017, doi: 10.3390/s17020307.
- [8] K. Liu, C. Hsieh, S. J. Hsu, and C. Chan, "Impact of Sampling Rate on Wearable-Based Fall Detection Systems Based on Machine Learning Models," *IEEE Sensors Journal*, vol. 18, no. 23, pp. 9882-9890, 2018, doi: 10.1109/JSEN.2018.2872835.
- [9] K. Liu, C. Hsieh, H. Huang, S. J. Hsu, and C. Chan, "An Analysis of Segmentation Approaches and Window Sizes in Wearable-Based Critical Fall Detection Systems With Machine Learning Models," *IEEE Sensors Journal*, vol. 20, no. 6, pp. 3303-3313, 2020, doi: 10.1109/JSEN.2019.2955141.
- [10] G. L. Santos, P. T. Endo, K. H. d. C. Monteiro, E. d. S. Rocha, I. Silva, and T. Lynn, "Accelerometer-Based Human Fall Detection Using Convolutional Neural Networks," *Sensors*, vol. 19, no. 7, p. 1644, 2019. [Online].
- [11] F. Luna-Perejón, M. J. Domínguez-Morales, and A. Civit-Balcells, "Wearable Fall Detector Using Recurrent Neural Networks," *Sensors*, vol. 19, no. 22, p. 4885, 2019. [Online].
- [12] C. Tan, F. Sun, T. Kong, W. Zhang, C. Yang, and C. Liu, "A survey on deep transfer learning," in *International conference on artificial neural networks*, 2018: Springer, pp. 270-279.
- [13] C.-F. Liao, Y. Tsao, H.-Y. Lee, and H.-M. Wang, "Noise Adaptive Speech Enhancement Using Domain Adversarial Training," *Proc. Interspeech 2019*, pp. 3148-3152, 2019.
- [14] Y. Zhang, R. Barzilay, and T. Jaakkola, "Aspect-augmented adversarial networks for domain adaptation," *Transactions of the Association for Computational Linguistics*, vol. 5, pp. 515-528, 2017.
- [15] A. Chadha and Y. Andreopoulos, "Improved Techniques for Adversarial Discriminative Domain Adaptation," *IEEE Transactions on Image Processing*, vol. 29, pp. 2622-2637, 2020.
- [16] Y. Ganin *et al.*, "Domain-adversarial training of neural networks," *The Journal of Machine Learning Research*, vol. 17, no. 1, pp. 2096-2030, 2016.
- [17] E. Casilari, J.-A. Santoyo-Ramón, and J.-M. Cano-García, "Analysis of Public Datasets for Wearable Fall Detection Systems," *Sensors*, vol. 17, no. 7, p. 1513, 2017. [Online].
- [18] L. Martínez-Villaseñor, H. Ponce, J. Brieva, E. Moya-Albor, J. Núñez-Martínez, and C. Peñafort-Asturiano, "UP-Fall Detection Dataset: A Multimodal Approach," *Sensors*, vol. 19, no. 9, p. 1988, 2019. [Online].
- [19] E. Casilari, J. A. Santoyo-Ramón, and J. M. Cano-García, "UMAFall: A Multisensor Dataset for the Research on Automatic Fall Detection," *Procedia Computer Science*, vol. 110, pp. 32-39, 2017/01/01/ 2017, doi: <https://doi.org/10.1016/j.procs.2017.06.110>.
- [20] A. T. Özdemir and B. Barshan, "Detecting Falls with Wearable Sensors Using Machine Learning Techniques," *Sensors*, vol. 14, no. 6, pp. 10691-10708, 2014. [Online].
- [21] D. P. Kingma and J. Ba, "Adam: A method for stochastic optimization," *arXiv preprint arXiv:1412.6980*, 2014.
- [22] L. v. d. Maaten and G. Hinton, "Visualizing data using t-SNE," *Journal of machine learning research*, vol. 9, no. Nov, pp. 2579-2605, 2008.
- [23] O. Steven Eyobu and D. S. Han, "Feature Representation and Data Augmentation for Human Activity Classification Based on

- Wearable IMU Sensor Data Using a Deep LSTM Neural Network," *Sensors*, vol. 18, no. 9, p. 2892, 2018. [Online].
- [24] S. Ruder, "An overview of multi-task learning in deep neural networks," *arXiv preprint arXiv:1706.05098*, 2017.
- [25] F. Sung, Y. Yang, L. Zhang, T. Xiang, P. H. Torr, and T. M. Hospedales, "Learning to compare: Relation network for few-shot learning," in *Proceedings of the IEEE Conference on Computer Vision and Pattern Recognition*, 2018, pp. 1199-1208.
- [26] J. Klenk *et al.*, "The FARSEEING real-world fall repository: a large-scale collaborative database to collect and share sensor signals from real-world falls," *European Review of Aging and Physical Activity*, vol. 13, no. 1, p. 8, 2016/10/30 2016